Communication

Length-Irrelevant Dual-Polarized Antenna Based on Antiphase Epsilon-Near-Zero Mode

Hao Li, Ziheng Zhou, and Yue Li

***Abstract*— In this communication, a novel dual-polarized (DP) epsilon-near-zero (ENZ) antenna is proposed with its operating frequencies independent of lengths for both polarizations. To obtain a DP implementation of ENZ antenna, an antiphase ENZ (AP-ENZ) mode is used based on a slot-fed substrate-integrated waveguide (SIW) antenna at its cutoff frequency, in which the electric field presents a sign-function-like distribution, presenting a fixed operating frequency independent on length. The proposed DP length-irrelevant antenna design is composed of a cross-shaped SIW operating on two orthogonal AP-ENZ modes, which are excited by a cavity-backed cross-shaped slot with good port isolation. The SIW lengths for both polarizations can be tuned independently without disturbing the operation frequency with controllable radiation patterns. To be specific, we study two cases of different lengths where sidelobe elimination and high gain radiation are realized, respectively. To verify this design, two antenna prototypes Ant. 1 and Ant. 2 are fabricated and tested, exhibiting agreements between simulation and experiment. The proposed Ant. 1 presents no sidelobes at 2.42 GHz while Ant. 2 shows a high gain of 10.56 dBi from 2.45 to 2.55 GHz. The proposed design method enables antennas with a variety of radiation patterns to be designed at a fixed frequency and both symmetric and asymmetric patterns for DP antennas. It also inspires the design of a flexible antenna with unchanged operating frequency when folded in both dimensions.**

***Index Terms*— Antenna diversity, antenna feed, antenna radiation patterns, antiphase epsilon-near-zero (AP-ENZ) antennas.**

I. Introduction

Polarization diversity antenna is widely utilized in modern wireless communication systems to deal with depolarization mismatch caused by scatterings and diffractions of irregular objects in the channel [1]. In this technology, multiple antennas with different polarizations are used [2]–[4]. A conventional design now widely used in base stations is a dual-polarized (DP) antenna with broadside radiation patterns for both $\pm 45^\circ$ polarizations [5]–[8]. In these antenna designs, two dipole antenna elements of half-wavelength lengths are placed orthogonally. Other DP implementations are based on the degenerated modes of symmetrically shaped patch antennas [9], dielectric resonator antennas [10], and slot antennas [11]. All these works provide identical beams for both polarizations. Besides these, DP antennas with asymmetrically adjustable radiation patterns for two polarizations, if exist, offer more possibilities for polarization diversity of channels with unequal propagation characteristics.

Manuscript received April 15, 2021; revised June 9, 2021; accepted June 27, 2021. Date of publication July 26, 2021; date of current version January 11, 2022. This work was supported in part by the National Natural Science Foundation of China under Grant 62022045, in part by the Beijing Nova Program of Science and Technology under Grant Z191100001119082, in part by the Youth Top Program of Beijing Outstanding Talent Funding Project, and in part by the National Key Research and Development Program of China under Grant 2018YFB1801603. *(Corresponding author: Yue Li.)*

The authors are with the Department of Electronic Engineering, Beijing National Research Center for Information Science and Technology, Tsinghua University, Beijing 100084, China (e-mail: lyee@tsinghua.edu.cn).

Color versions of one or more figures in this communication are available at https://doi.org/10.1109/TAP.2021.3098548.

Digital Object Identifier 10.1109/TAP.2021.3098548

The recent progress made in the field of metamaterials inspires novel antenna designs [13]–[18]. Among these, the epsilon-near-zero (ENZ) material has been attracting research interests for decades due to various interesting phenomena resulted from the ultralow permittivity [19]–[22]. In this medium, the electromagnetic wave has infinite wavelength and zero propagation constant at nonzero frequencies, supporting a zeroth-order resonance (ZOR) which has a resonant frequency independent of the geometric parameters. With the assistant of ZOR, a series of novel antennas are designed to have enhanced gains [23]–[26], miniaturized sizes [27]–[29], wide bandwidths [30]–[32], and shaped radiation patterns [33]. In [34] and [35], antennas with length-invariant frequencies are proposed using the ENZ modes in which the electric fields are uniformly distributed thus generating differential beams. In terms of applications, both wearable devices and biomedical uses need flexible antennas operating under deformations [36], while previous works prove that folding an antenna along the resonant length may cause an obvious frequency shift [37]. A ZOR antenna implemented on flexible substrate is adopted in [38] to solve this problem. However, when stretching or bending this antenna along the transverse direction of the substrate-integrated waveguide (SIW), the operating frequency may be disturbed. Therefore, it only maintains an unchanged frequency when folded along one direction.

Since most of the ZOR antennas operate based on a uniformly distributed electric field, this mode is not orthogonal to itself after a 90° rotation, unlike ordinary resonant modes used in DP antennas. In other words, simply combining two perpendicular zeroth-order resonators cannot realize a DP ZOR antenna due to poor isolations. Some inspirations may be found in [35] where a 180° phase shift is generated by a half-wavelength ceramic block thus generating an odd-symmetric ZOR, which is orthogonal to itself after a 90° rotation. However, the ceramic block introduces new structural difficulties on DP implementation. Therefore, designing a DP ZOR antenna remains a tough task.

In this communication, a general concept of DP ENZ antenna is proposed with operating frequencies not related to its lengths for both polarizations. Different from the previously used ENZ modes, an antiphase ENZ (AP-ENZ) mode with a 180° phase shift is excited by a slot in the SIW cavity, as depicted in Fig. 1. A sign-function-like distribution of the electric fields in this mode results in a length-invariant operating frequency together with two in-phase magnetic currents at both ends, generating a broadside radiation pattern. Based on the studies of this exotic resonance, a DP antenna is composed using a cross-shaped SIW, which is fed by a cavity-backed cross slot. The length of SIW's each arm can be tuned independently with an unchanged frequency, resulting in a controllable gain for both polarizations and enabling asymmetrically adjustable radiation patterns. Two antenna prototypes, denoted as Ant. 1 and Ant. 2, have been fabricated and tested under the same proposed designing method, aiming at realizing sidelobe elimination and high gain, respectively. With the capability of realizing various radiation

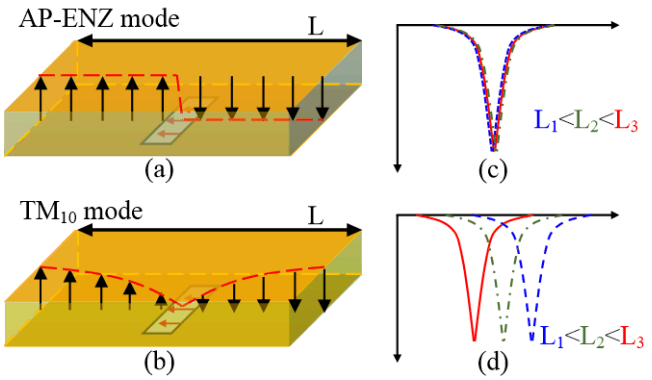

Fig. 1. Comparison between the TM_{10} mode used in conventional patch antennas and the AP-ENZ mode used in the proposed antenna design: (a) proposed AP-ENZ mode, (b) TM_{10} mode, and (c) and (d) reflection coefficients of these two kinds of resonances.

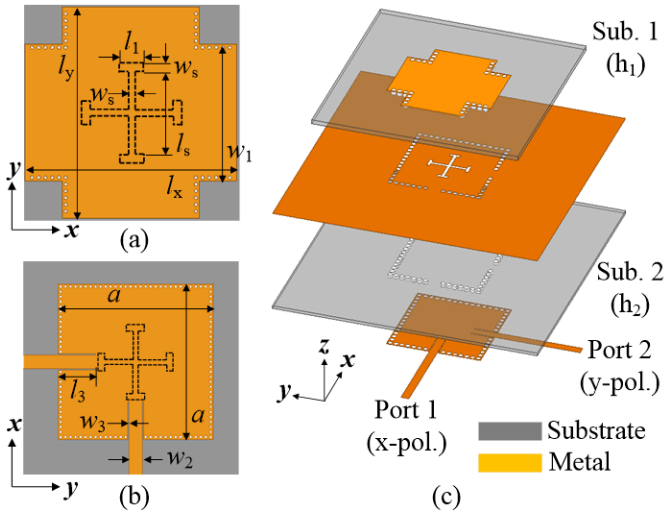

Fig. 2. Configuration of the DP ENZ antenna Ant. 1 from (a) top view, (b) bottom view, and (c) exploded view.

properties and superior performances in some specific cases, the proposed design is competent for WLAN or other wireless communication applications. In addition to the polarization diversity property, we also schematically demonstrate that this antenna configuration is helpful for designing a flexible antenna that can be stretched or bent in both directions without influences on the operating frequency.

II. Operating Principle and DP Antenna Design

First, the resonant mode is analyzed in the effective ENZ medium fed by a slot. It is proved in [21] that a rectangular waveguide exhibits a plasmonic material with an effective permittivity described by the Drude model, which is written as $\varepsilon_{\text{eff}} = \varepsilon_{\text{r}} - 4c^2 f^2/W^2$. Here W is the width of the waveguide and ε_{r} is the relative permittivity of the inside dielectrics. It can be derived that at the cutoff frequency f_{c10} of the TE_{10} mode, the effective permittivity is zero so that such a waveguide shows the same propagating characteristics with an ENZ medium at f_{c10} including an infinite wavelength and a zero propagating constant β. Within this medium, a magnetic current source, i.e., a slot, can excite a sign-function-like electric field distribution within the ENZ medium in this case. To distinguish this mode from the previously-used ENZ mode, it is defined as the AP-ENZ mode because the electric fields are out of phase on two sides of the slot. Compared with the conventional TM_{10} mode of a patch antenna shown in Fig. 1(b), it can be seen that a sharp inverse of the electric field exists near the slot instead of a sinusoidal distribution within the whole cavity. This difference results in different frequency responses of the AP-ENZ mode and the TM_{10} mode. As depicted in Fig. 1(c) and (d), the resonant frequency of the AP-ENZ mode keeps invariant under different length L while that of the TM_{10} mode varies with L. In addition, both AP-ENZ and TM_{10} mode can be used for broadside radiation patterns because they both generate two in-phase magnetic currents at both cavity ends.

With the analysis of the AP-ENZ mode, a DP antenna is composed and its configuration is shown in Fig. 2. As shown in Fig. 2(a), the top substrate layer, named as Substrate 1, contains a cross-shaped open-ended SIW which has two arms both operating at the cutoff frequency. This SIW antenna is coupled to a cavity in Substrate 2 through a slot-shaped Jerusalem cross. Two 50 Ω microstrip lines are utilized for feeding both polarizations. The panel on the bottom is depicted in Fig. 2(b). Both substrates are F4B with a permittivity of 2.6 and a loss tangent of 0.002. All the metal vias share the same diameter of 1.0 mm in this structure and other geometric parameters are listed in Table I. According to [39], the SIW is equivalent to a rectangular waveguide with an effective width W_{eff}, which is calculated as $W_{\text{eff}} = w_1 - d^2/(0.95p_1)$. In this formula, w_1 is the actual width of the SIW and the parameters d and p_1 represent the diameters and pitch of the vias, respectively. Based on this structure, simulations are launched to study the characteristics of the proposed AP-ENZ mode. The simulated reflection coefficients and isolations are shown in Fig. 3 when the length of the SIW l_x varies from 0.46 λ_0 (57.4 mm) to 0.70 λ_0 (87.4 mm) while l_y is kept the same to be 0.46 λ_0. S_{22} is omitted in each case for brevity. In contrast to the TM_{11} mode, the resonant frequency of the AP-ENZ mode is always 2.42 GHz which is independent of the length of the SIW. At this frequency, the field distributions inside the SIW are also simulated and depicted in Fig. 4. As shown in Fig. 4(a), the electric field keeps a constant magnitude along l_x within the SIW while its direction on one

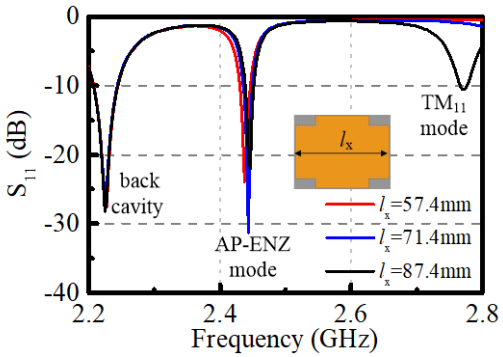

Fig. 3. Simulated S_{11} of the example antenna in variation of the length l_x.

TABLE I
Detailed Dimensions

Parameter	Value (mm)	Parameter	Value (mm)	Parameter	Value (mm)
h_1	2.0	h_2	2.0	w_1	38.4
w_2	5.4	w_3	0.5	w_4	62.5
w_5	100.0	w_s	2.0	l_1	7.0
l_2	75.0	l_3	15.0	l_4	17.0
l_s	25.0	a	72.0	l_x	65.4
l_y	65.4				

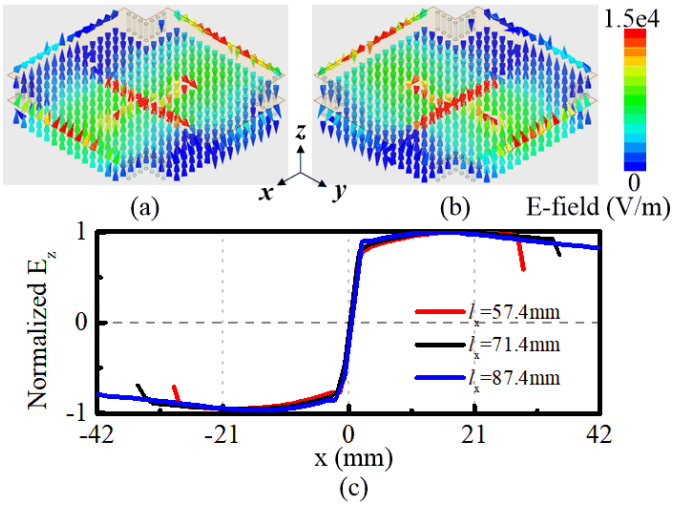

Fig. 4. Simulated electric field distribution of the antenna: (a) excited by Port 1, (b) excited by Port 2, and (c) normalized electric field along z-direction on the center plane at different locations along the x-axis with variation to the total length l_x.

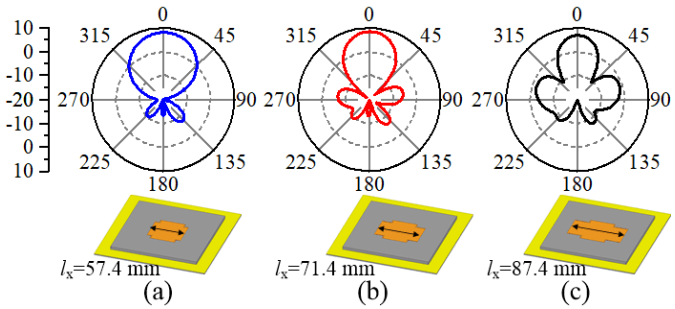

Fig. 5. (a)–(c) X-polarized radiation patterns at 2.42 GHz in E-plane with different l_x.

side of the feeding slot differs from the other, demonstrating a 180° phase shift at the feeding point. To show the electric field distribution clearly, the vector electric field on the center plane is also presented in Fig. 4(b) where a sign-function-like distribution is observed of the AP-ENZ mode. To give a more quantitive illustration, the z-polarized electric fields in the center plane fed by Port 1 in three different cases are all plotted in Fig. 4(c), demonstrating a sign-function-like distribution.

The length-invariance offers opportunities to independently control the radiation pattern of each polarization simply by stretching or shortening the corresponding arm. The radiation patterns of antennas with different l_x and l_y are investigated and plotted in Fig. 5. It can be concluded that a narrower beamwidth together with a higher sidelobe level (SLL) are both obtained for either x- or y-polarization with the increasing of l_x or l_y at a fixed frequency. When the length equals 0.6 λ_0, the antenna's gain reached its maximum which is about 10 dBi, higher than the typical value of a patch antenna. This gain enhancement is achieved at the expense of an increase in the SLL. Moreover, the radiation pattern of both polarizations can be asymmetrically tuned using different arm lengths. Another important issue is the impedance bandwidth of the antenna. Although the bandwidth of the antenna is configured by Fig. 2, several methods are available for a relatively wider bandwidth. Two of the most common methods are increasing the height of the SIW and replacing the dielectric substrate by air. Fig. 6 depicts the reflection coefficients of three specific cases with different heights and substrate types,

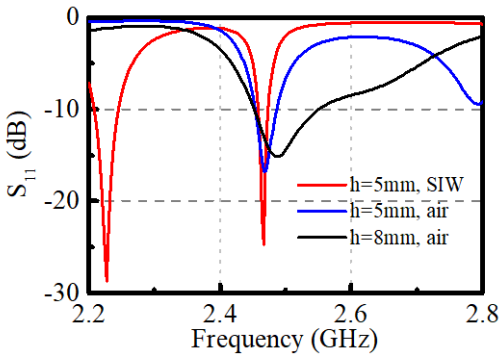

Fig. 6. Simulated reflection coefficients with variety to the height and the substrates of the antenna.

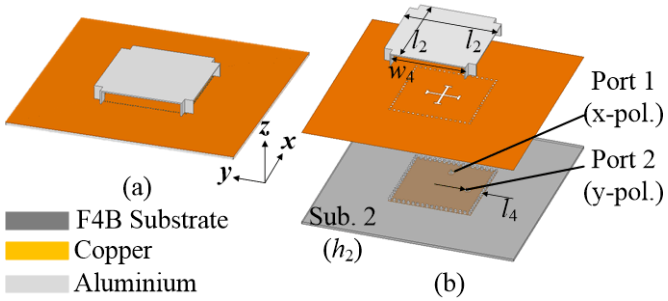

Fig. 7. Configuration of the proposed DP antenna Ant. 2 from (a) perspective and (b) exploded view.

demonstrating that both a thicker profile and a lower dielectric constant are helpful for bandwidth enhancement. Inspired by this critical result, another DP ENZ antenna, named Ant. 2, is designed by replacing the top substrate by a metallic cross-shaped waveguide with a 1 mm thickness. Fig. 7 shows the configuration of Ant. 2, in which the geometric parameter of the Jerusalem cross is inherited from Ant. 1. The coaxial feed is used rather than the microstrip line here. Other dimensions are also presented in Table I. The length of each arm equals 0.62 λ_0, aimed at obtaining a high broadside gain.

This proposed antenna's configuration and principle may be used to implement a foldable antenna on flexible substrates like PDMS, SU-8, or liquid crystal polymers (LCPs). Since a flexible antenna may suffer frequency shift when it is stretched or folded along the resonant length, it is difficult to achieve a completely folding-independent flexible antenna. A possible solution is depicted schematically in Fig. 8. The center of the cross-shaped SIW, together with the feeding structures is composed of a rigid substrate while the four arms are based on a flexible substrate that can be deformed. According to the discussions in former paragraphs, this antenna can maintain a fixed operating frequency when its arms are stretched or bent in either x- or y-direction as shown in Fig. 8(b) and (c). In both cases, the gain might be changed but the radiation pattern remains a broadside one, demonstrating a deformation-independent feature.

III. Antenna Fabrication and Measurements

To validate the proposed DP ENZ antenna design, two antenna prototypes shown in Figs. 2 and 7 are fabricated and tested. For Ant. 1, we use the standard print circuit board (PCB) process for each layer of substrate and assemble them together using 9 Nylon screws. Both substrates are F4B with a per-

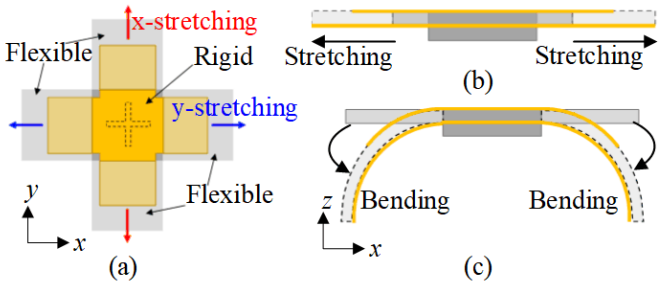

Fig. 8. Schematic graph of the 2-D foldable antenna's configuration based on the proposed antenna in the communication from (a) top view and (b) and (c) side view when the antenna is stretched or bent.

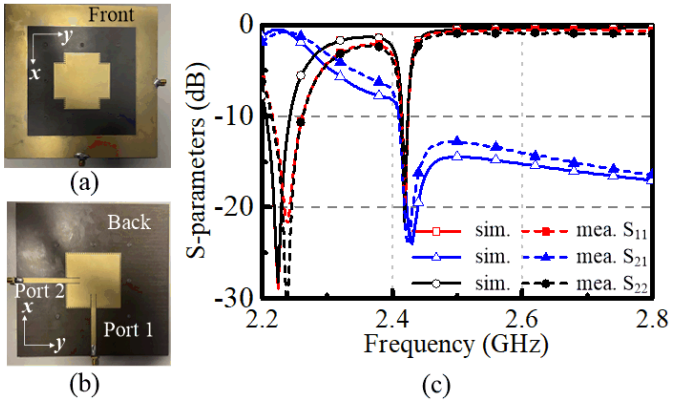

Fig. 9. (a) Photograph of Ant. 1 from the front view, (b) photograph of Ant. 1 from the back view, and (c) simulated and measured S-parameters of Ant. 1.

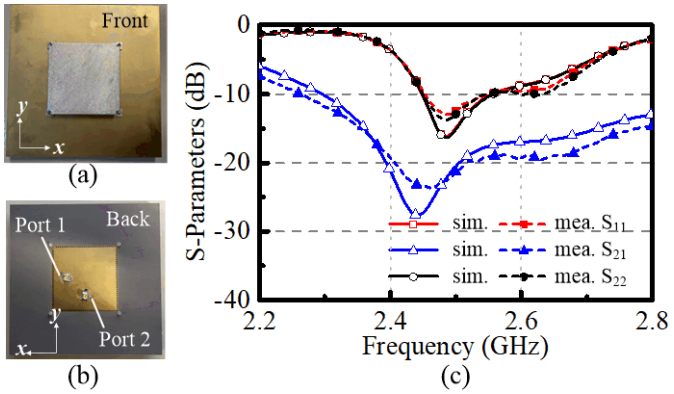

Fig. 10. (a) Photograph of Ant. 2 from the front view, (b) photograph of Ant. 1 from the back view, and (c) simulated and measured S-parameters of Ant. 2.

mittivity of 2.6 and a loss tangent of 0.002. Ant. 2 contains two major parts using different fabrication techniques. The metallic waveguide is fabricated using computer numerical controlled (CNC) machining and assembled using 4 Nylon screws with the PCB substrate.

The S-parameters of the fabricated prototype are measured using the vector network analyzer Agilent N9917A. Fig. 9 shows the photographs and S-parameters of Ant. 1, demonstrating an impedance bandwidth of 2.42–2.43 GHz and isolations higher than 15.5 dB. For Ant. 2, the photographs and S-parameters are exhibited in Fig. 10. From Fig. 10(c), one can find that the impedance bandwidth is 2.45–2.55 GHz, which is enough for applications including WLAN. The in-band isolation is higher than 19.0 dB.

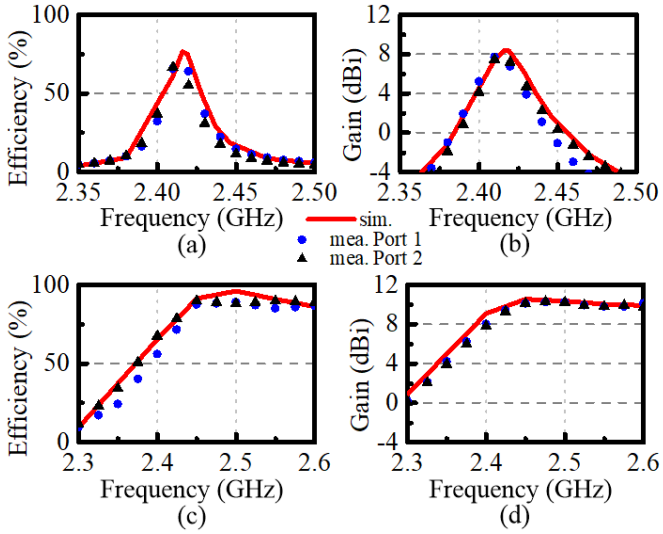

Fig. 11. Simulated and measured (a) efficiencies and (b) gains of Ant. 1. (c) Efficiencies and (d) gains of Ant. 2.

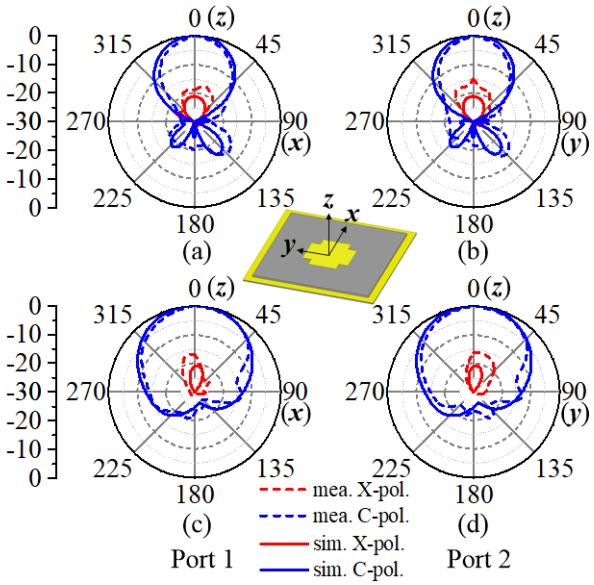

Fig. 12. Simulated and measured normalized radiation patterns of the proposed prototype Ant. 1 at 2.42 GHz in *xz*-plane excited from (a) Port 1 and (b) Port 2. And in *yz*-plane excited from (c) Port 1 and (d) Port 2.

The radiation performances are also tested in an anechoic chamber. Fig. 11 shows all the simulated and measured gains and radiation efficiencies of both antenna prototypes. As seen from Fig. 11(a) and (b), Ant. 1 suffers from a relatively high dielectric loss and performs a radiation efficiency of 77% according to simulations and 73.1% according to measurement. According to Fig. 11(c) and (d), Ant. 2 achieves a high gain of 10.56 dBi by simulation and 10.2 dBi by measurements. The radiation efficiency is measured to be 88%. The normalized radiation patterns of Ant. 1 in *xz*-plane and *yz*-plane are measured and plotted in Fig. 12 for both polarizations. It can be seen that a broadside radiation pattern without sidelobe is obtained for each polarization and the measured ones agree with the simulations well. In contrast, sidelobes exist in the radiation pattern of Ant. 2, as shown in Fig. 13. The simulated and measured SLL of Ant. 2 is −9.5 and −7.6 dB, respectively. Both the simulations and measurements show that our proposed designing method enables antennas designed with

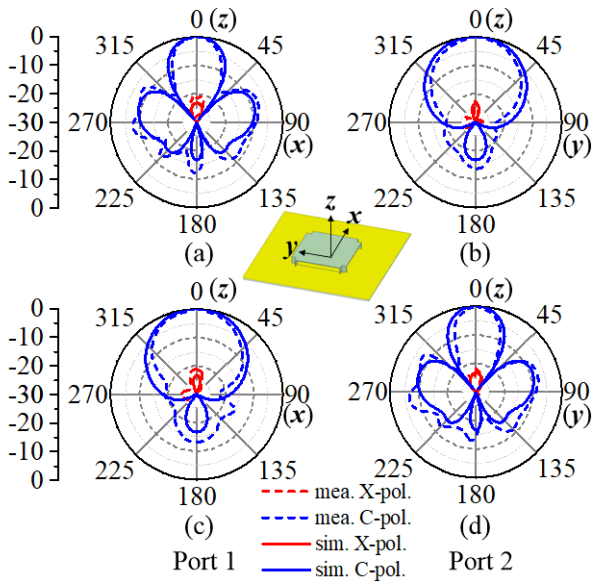

Fig. 13. Simulated and measured normalized radiation patterns of the proposed prototype Ant. 2 at 2.45 GHz in *xz*-plane excited from (a) Port 1 and (b) Port 2. And in *yz*-plane excited from (c) Port 1 and (d) Port 2.

TABLE II

COMPARISON AMONG THE PROPOSED DESIGN AND OTHER ZOR ANTENNAS

Ref.	Pol.	BW (%)	Size (λ_0^3)	Radiation pattern	Max. Gain (dBi)
[34] Ant.1	SP	0.5	0.27*1.32*0.02	Broadside	8.37
[34] Ant.2	SP	0.5	0.27*1.05*0.02	Monopolar	7.01
[35]	SP	1.7	0.35*0.5*0.05	Broadside	9.6
[40]	SP	0.7	0.53*0.53*0.016 (at f_2)	Monopolar	1.3
[41]	SP	3.3	0.19*0.29*0.06	Broadside	4.7
[42]	SP	10.3	0.19*0.33*0.01	Dipolar	2.3
Ant. 1	**DP**	**0.4**	**0.51*0.51*0.03**	**Broadside**	**8.10**
Ant. 2	**DP**	**4.0**	**0.62*0.62*0.08**	**Broadside**	**10.56**

various radiation performances, including but not limited to sidelobe elimination and high gain radiation.

Table II lists a comparison among the proposed antenna design and other state-of-art ZOR antennas. We believe that these ZOR antennas have the potential to compose a length-invariant antenna for at least a single polarization. It should be stressed that these are the first DP ZOR antennas, which broaden the applications of ZOR mode. In terms of antenna performances, the proposed Ant. 2 exhibits a higher gain than other designs. Moreover, since ZOR usually suffers from high Q-factor, a 4.0% impedance bandwidth is also a relatively wide value.

IV. CONCLUSION

In this communication, a novel DP ENZ antenna with length-independent operating frequencies for both polarizations is proposed based on a new resonance, which is defined as the AP-ENZ mode, in a slot-fed SIW at its cutoff frequency. By using a cross-shaped SIW with four open ends fed by a cross slot, the AP-ENZ mode is excited for both x- and y-polarizations. By changing the length of each arm, the proposed antenna designing method enables a variety of radiation patterns for each polarization. Two specific antenna prototypes with different lengths are designed, fabricated, and tested in which Ant. 1 has no sidelobes while Ant. 2 is with a gain of 10.56 dBi and a fractional bandwidth of 2.45–2.55 GHz. With the merits of asymmetrically controllable gains at a fixed frequency and realizing higher gain than ordinary designs, the proposed DP antenna can be deployed in sensing systems, energy harvesting, and wireless communication applications including WLAN with the demands of adaptively tunable radiation performance. Furthermore, it also shows plenty of potentials to be converted into a flexible antenna, which has a fixed operating frequency under two-dimensional deformations as demanded by wearable and biomedical applications.

REFERENCES

[1] R. G. Vaughan, "Polarization diversity in mobile communications," *IEEE Trans. Veh. Technol.*, vol. 39, no. 3, pp. 177–186, May 1990.
[2] R. J. Bolt *et al.*, "Characterization of a dual-polarized connected-dipole array for Ku-band mobile terminals," *IEEE Trans. Antennas Propag.*, vol. 64, no. 2, pp. 591–598, Feb. 2016.
[3] M. Notaros, M. Ignatenko, and D. S. Filipovic, "Miniaturization of a high-frequency dual linearly polarized dipole for vehicular communications," in *Proc. IEEE Int. Symp. Antennas Propag. (APSURSI)*, Fajardo, Jun. 2016, pp. 1751–1752.
[4] O. Jo, J.-J. Kim, J. Yoon, D. Choi, and W. Hong, "Exploitation of dual-polarization diversity for 5G millimeter-wave MIMO beamforming systems," *IEEE Trans. Antennas Propag.*, vol. 65, no. 12, pp. 6646–6655, Dec. 2017.
[5] L.-H. Wen *et al.*, "Compact dual-polarized shared-dipole antennas for base station applications," *IEEE Trans. Antennas Propag.*, vol. 66, no. 12, pp. 6826–6834, Dec. 2018.
[6] R. Wu and Q.-X. Chu, "A compact, dual-polarized multiband array for 2G/3G/4G base stations," *IEEE Trans. Antennas Propag.*, vol. 67, no. 4, pp. 2298–2304, Apr. 2019.
[7] Y. He, Y. Yue, and Z. Shen, "A novel broadband dual-polarized antenna element for LTE 700 MHz/GSM 850 MHz/GSM 900 MHz applications," *IEEE Access*, vol. 4, pp. 4321–4326, 2016.
[8] W. Yang and Y. Pan, "A wideband dual-polarized dipole antenna with folded metallic plates," *IEEE Antennas Wireless Propag. Lett.*, vol. 17, no. 10, pp. 1797–1801, Oct. 2018.
[9] H.-W. Lai and K.-M. Luk, "Dual polarized patch antenna fed by meandering probes," *IEEE Trans. Antennas Propag.*, vol. 55, no. 9, pp. 2625–2627, Sep. 2007.
[10] Y. X. Sun and K. W. Leung, "Dual-band and wideband dual-polarized cylindrical dielectric resonator antennas," *IEEE Antennas Wireless Propag. Lett.*, vol. 12, pp. 384–387, 2013.
[11] X. Qin and Y. Li, "Compact dual-polarized cross-slot antenna with colocated feeding," *IEEE Trans. Antennas Propag.*, vol. 67, no. 11, pp. 7139–7143, Nov. 2019.
[12] C. A. Balanis, *Antenna Theory: Analysis and Design*, 2nd ed. New York, NY, USA: Wiley, 1997.
[13] J. B. Pendry, "Negative refraction makes a perfect lens," *Phys. Rev. Lett.*, vol. 85, no. 18, pp. 3966–3969, Oct. 2000.
[14] D. R. Smith, W. J. Padilla, D. C. Vier, S. C. Nemat-Nasser, and S. Schultz, "Composite medium with simultaneously negative permeability and permittivity," *Phys. Rev. Lett.*, vol. 84, no. 18, pp. 4184–4187, May 2000.
[15] N. Engheta and R. W. Ziolkowski, Eds., *Metamaterials: Physics and Engineering Explorations*. Hoboken, NJ, USA: Wiley, 2006.
[16] N. Zhu and R. W. Ziolkowski, "Active metamaterial-inspired broadband-width, efficient, electrically small antennas," *IEEE Antennas Wireless Propag. Lett.*, vol. 10, pp. 1582–1585, 2011.
[17] J. Zhu, M. A. Antoniades, and G. V. Eleftheriades, "A compact tri-band monopole antenna with single-cell metamaterial loading," *IEEE Trans. Antennas Propag.*, vol. 58, no. 4, pp. 1031–1038, Apr. 2010.
[18] J. Wang *et al.*, "Metantenna: When metasurface meets antenna again," *IEEE Trans. Antennas Propag.*, vol. 68, no. 3, pp. 1332–1347, Mar. 2020.
[19] M. Silveirinha and N. Engheta, "Tunneling of electromagnetic energy through subwavelength channels and bends using ε-near-zero materials," *Phys. Rev. Lett.*, vol. 97, no. 15, Oct. 2006, Art. no. 157403.
[20] I. Liberal, A. M. Mahmoud, and N. Engheta, "Geometry-invariant resonant cavities," *Nature Commun.*, vol. 7, no. 1, p. 10989, Mar. 2016.
[21] Y. Li, I. Liberal, C. D. Giovampaola, and N. Engheta, "Waveguide metatronics: Lumped circuitry based on structural dispersion," *Sci. Adv.*, vol. 2, no. 6, Jun. 2016, Art. no. e1501790.

[22] I. Liberal, A. M. Mahmoud, Y. Li, B. Edwards, and N. Engheta, "Photonic doping of epsilon-near-zero media," *Science*, vol. 355, no. 6329, pp. 1058–1062, Mar. 2017.
[23] S. Enoch, G. Tayeb, P. Sabouroux, N. Guérin, and P. Vincent, "A metamaterial for directive emission," *Phys. Rev. Lett.*, vol. 89, no. 21, Nov. 2002, Art. no. 213902.
[24] E. Forati, G. W. Hanson, and D. F. Sievenpiper, "An epsilon-near-zero total-internal-reflection metamaterial antenna," *IEEE Trans. Antennas Propag.*, vol. 63, no. 5, pp. 1909–1916, May 2015.
[25] B. Zhou and T. J. Cui, "Directivity enhancement to Vivaldi antennas using compactly anisotropic zero-index metamaterials," *IEEE Antennas Wireless Propag. Lett.*, vol. 10, pp. 326–329, 2011.
[26] H. Zhou *et al.*, "A novel high-directivity microstrip patch antenna based on zero-index metamaterial," *IEEE Antennas Wireless Propag. Lett.*, vol. 8, pp. 538–541, 2009.
[27] S. K. Sharma, A. Gupta, and R. K. Chaudhary, "Epsilon negative CPW-fed zeroth-order resonating antenna with backed ground plane for extended bandwidth and miniaturization," *IEEE Trans. Antennas Propag.*, vol. 63, no. 11, pp. 5197–5203, Nov. 2015.
[28] P.-L. Chi and Y.-S. Shih, "Compact and bandwidth-enhanced zeroth-order resonant antenna," *IEEE Antennas Wireless Propag. Lett.*, vol. 14, pp. 285–288, 2015.
[29] E. P. Jee and Y. Jee, "Compact dual-band CPW-fed zeroth-order resonant monopole antennas," *IEEE Antennas Wireless Propag. Lett.*, vol. 11, pp. 712–715, 2012.
[30] K. Wei, Z. Zhang, Z. Feng, and M. F. Iskander, "A wideband MNG-TL dipole antenna with stable radiation patterns," *IEEE Trans. Antennas Propag.*, vol. 61, no. 5, pp. 2418–2424, May 2013.
[31] A. Jafargholi and M. H. Mazaheri, "Broadband microstrip antenna using epsilon near zero metamaterials," *IET Microw., Antennas Propag.*, vol. 9, no. 14, pp. 1612–1617, Nov. 2015.
[32] B.-J. Niu, Q.-Y. Feng, and P.-L. Shu, "Epsilon negative zeroth- and first-order resonant antennas with extended bandwidth and high efficiency," *IEEE Trans. Antennas Propag.*, vol. 61, no. 12, pp. 5878–5884, Dec. 2013.
[33] Z. Hao Jiang and D. H. Werner, "Anisotropic metamaterial lens with a monopole feed for high-gain multi-beam radiation," in *Proc. IEEE Int. Symp. Antennas Propag. (APSURSI)*, Spokane, WA, USA, Jul. 2011, pp. 1346–1349.
[34] Z. Zhou and Y. Li, "Effective epsilon-near-zero (ENZ) antenna based on transverse cutoff mode," *IEEE Trans. Antennas Propag.*, vol. 67, no. 4, pp. 2289–2297, Apr. 2019.
[35] Z. Zhou and Y. Li, "A photonic-doping-inspired SIW antenna with length-invariant operating frequency," *IEEE Trans. Antennas Propag.*, vol. 68, no. 7, pp. 5151–5158, Jul. 2020.
[36] A. Kiourti and J. L. Volakis, "Stretchable and flexible E-fiber wire antennas embedded in polymer," *IEEE Antennas Wireless Propag. Lett.*, vol. 13, pp. 1381–1384, 2014.
[37] S. Alharbi and A. Kiourti, "Folding-dependent vs. folding-independent flexible antennas on E-textiles," in *Proc. IEEE Int. Symp. Antennas Propag. USNC-URSI Radio Sci. Meeting*, Atlanta, GA, USA, Jul. 2019, pp. 755–756.
[38] Z. Hu, C. Chen, Z. Zhou, and Y. Li, "An epsilon-near-zero-inspired PDMS substrate antenna with deformation-insensitive operating frequency," *IEEE Antennas Wireless Propag. Lett.*, vol. 19, no. 9, pp. 1591–1595, Sep. 2020.
[39] Y. Cassivi, L. Perregrini, P. Arcioni, M. Bressan, K. Wu, and G. Conciauro, "Dispersion characteristics of substrate integrated rectangular waveguide," *IEEE Microw. Wireless Compon. Lett.*, vol. 12, no. 9, pp. 333–335, Sep. 2002.
[40] A. Mehdipour, T. A. Denidni, and A.-R. Sebak, "Multi-band miniaturized antenna loaded by ZOR and CSRR metamaterial structures with monopolar radiation pattern," *IEEE Trans. Antennas Propag.*, vol. 62, no. 2, pp. 555–562, Feb. 2014.
[41] S. Ko and J. Lee, "Hybrid zeroth-order resonance patch antenna with broad E-plane beamwidth," *IEEE Trans. Antennas Propag.*, vol. 61, no. 1, pp. 19–25, Jan. 2013.
[42] P.-W. Chen and F.-C. Chen, "Asymmetric coplanar waveguide (ACPW) zeroth-order resonant (ZOR) antenna with high efficiency and bandwidth enhancement," *IEEE Antennas Wireless Propag. Lett.*, vol. 11, pp. 527–530, 2012.